

Approximated Method Neglecting Coupling for Conformal Array

François Chauvet¹, Régis Guinvarc'h¹ and Marc Hélier²

¹ SONDRA, Supélec

3 rue Joliot-Curie, 91190 Gif-sur-Yvette France

francois.chauvet@supelec.fr, regis.guinvarch@supelec.fr

² Université Pierre et Marie Curie-Paris 6 /LISIF

3 rue Galilée, 94200 Ivry-sur-Seine France

marc.helier@upmc.fr

Abstract — Full modeling of large conformal array can be time and memory consuming. An approximated method that takes into account the vectorial nature of the radiated field is presented. The radiation characteristic of the array is obtained by means of the vectorial sum of each element radiation characteristic, rotated according to the orientation of the element. The coupling between elements will be evaluated in the case of interest: a conformal array on an inflatable structure. In the approximated method, coupling will be neglected in such a case. To illustrate the approach, a spiral antenna will be chosen and modeled with MoM. Finally, array radiation patterns obtained by the approximated method will be compared with a full wave MoM to validate our method, in the case of a simplified 1D circular array.

Keywords — Spiral antenna, coupling, wideband array, conformal antennas.

I. INTRODUCTION

A high altitude airship (HAA) offers great potential as a host platform for low frequency antenna array [1]. The main advantage is the large surface available, allowing good performances for applications like radar tracking and telecommunications at lower cost than satellites. The antenna array has to be conformed to the ellipsoidal shape of the airship hull and must fill wideband, low weight, low power, low profile conditions. The array lies on the side of the airship and must achieve a bandwidth centered on 500 MHz as well as digital beamforming capability. The unusual configuration of our array must be pointed out since we assume that no ground plane will be used because of low profile condition and because we assume that the equipment must lie outside the hull.

The usual modeling tool (FEKO) based on method of moments (MoM) is no longer appropriate to study such a

large array. Indeed, the number of antennas is too high and modeling becomes time and memory consuming.

However, it is possible to obtain the radiation characteristic of the array if the coupling between elements is low by making the sum of each element contributions [2]. Thus, only one radiation characteristic of an isolated element has to be computed by the MoM, reducing the computation time consequently.

Therefore, after presenting the approximated method based on rotation of the radiation characteristic and phase shift according to the position of each element. The choice of a radiating element will be explained and results of FEKO simulations of this antenna will be described.

Then coupling between array elements will be examined in the chosen frequency range at different array curvatures in order to quantify the effect of coupling.

Finally, considering a small array, radiation patterns obtained with exact method and computed with neglected coupling by the approximated method will be compared. Influence of the frequency and curvature will be investigated.

II. APPROXIMATED METHOD

In order to avoid the modeling of the full array, we assume that the radiated far field of the conformal array is the sum of the radiated far fields of each antenna element as it is usually assumed for classical planar array [3]. This assumption involves neglecting the coupling between elements. Thus, this method can be applied for any radiating element, as long as the coupling between elements of the array is low. This approach is expected to noticeably reduce the time consuming issue, since it is only necessary to model only one antenna element with an exact method before doing the sum of all elements of the array. The antenna must be modeled in its own environment in order to define its radiation characteristic.

First, phase shift between elements due to the distance from the phase reference are taken into account. Each element at position m is characterized by a translation vector δ_m (Fig. 1). Thus the components (E_θ , E_φ) of the array total far field \mathbf{E}^{tot} in the main coordinate system (\mathbf{e}_r , \mathbf{e}_θ , \mathbf{e}_φ) (Figure 2) can be expressed as a function of the \mathbf{E}_m far field radiated by element m , expressed in the main coordinate system as well,

$$\mathbf{E}^{\text{tot}}(\theta, \varphi) = \sum_{m=1}^N \exp(jk \vec{e}_r \cdot \vec{\delta}_m) \mathbf{E}_m(\theta, \varphi). \quad (1)$$

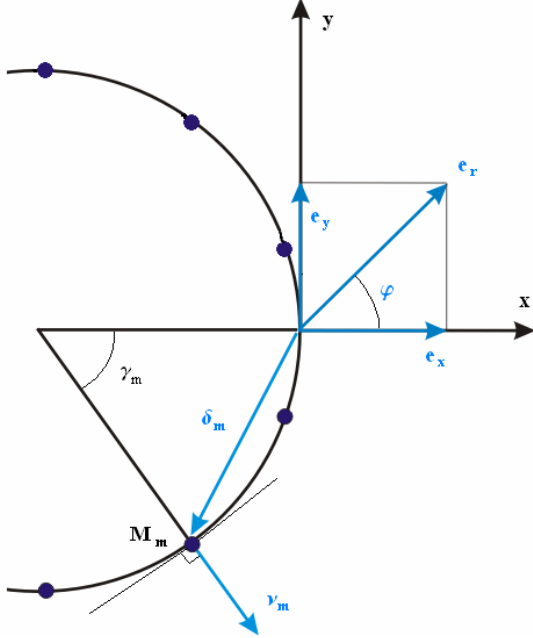


Fig. 1. Circular 1D conformal array configuration.

In order to obtain \mathbf{E}_m , the orientation of each antenna element has to be taken into account as it changes, in a given direction, magnitude, phase and polarization properties of the isolated element. FEKO gives far field results as (E'_θ , E'_φ) components of the element antenna far field \mathbf{E}' [4], at discrete values (θ' , φ') in the local coordinate system of an isolated element (\mathbf{e}'_r , \mathbf{e}'_θ , \mathbf{e}'_φ). The radiation characteristic \mathbf{E}' has to be expressed in the main coordinate system (\mathbf{e}_r , \mathbf{e}_θ , \mathbf{e}_φ). The orientation of each element is taken into account by means of a rotation matrix \mathbf{R} (see figure 2).

A general rotation \mathbf{R} can be written in terms of successive rotation matrix \mathbf{R}_z , \mathbf{R}_ξ , and $\mathbf{R}_{z'}$ [5], with the three rotation Euler angles γ , β , ψ , (see figure 3),

$$\mathbf{R} = \mathbf{R}_{z'}(\psi) \mathbf{R}_\xi(\beta) \mathbf{R}_z(\gamma). \quad (2)$$

To obtain the rotated radiation characteristic, we apply eq. (3), where \mathbf{E}_m has its components in the main coordinate system (\mathbf{e}_r , \mathbf{e}_θ , \mathbf{e}_φ)

$$\mathbf{E}_m(\theta, \varphi) = \mathbf{T}_2 \mathbf{R}_m \mathbf{T}_1 \mathbf{E}'(\theta', \varphi'). \quad (3)$$

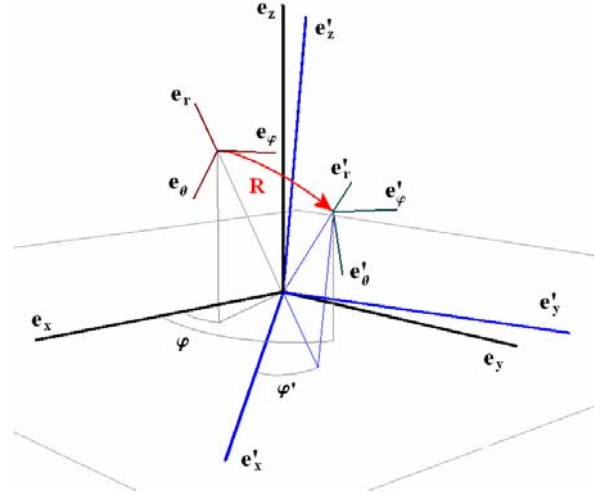


Fig. 2. Local coordinate system of an isolated element (\mathbf{e}'_r , \mathbf{e}'_θ , \mathbf{e}'_φ) and main coordinate system (\mathbf{e}_r , \mathbf{e}_θ , \mathbf{e}_φ) rotated by a rotation matrix \mathbf{R} .

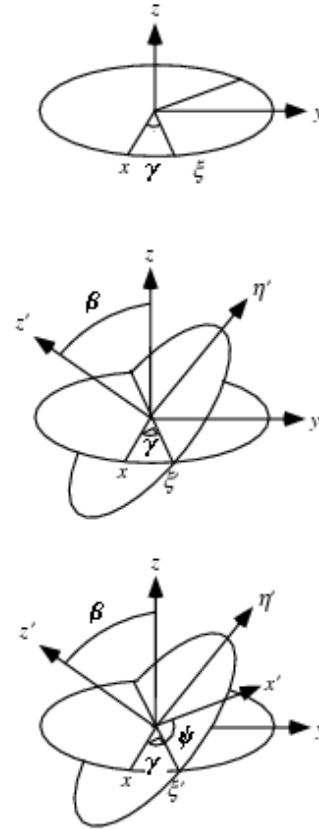


Fig. 3. Successive rotation matrix \mathbf{R}_z , \mathbf{R}_ξ , and $\mathbf{R}_{z'}$, with the three rotation Euler angles γ , β , ψ .

As rotation matrix, \mathbf{R}_m must be used in a cartesian coordinate system. Transformation matrix \mathbf{T}_1 from spherical to cartesian coordinate system and transformation matrix \mathbf{T}_2 from cartesian to spherical are required and given below

$$\mathbf{T}_1 = \begin{bmatrix} \sin \theta' \cos \varphi' & \cos \theta' \cos \varphi' & -\sin \varphi' \\ \sin \theta' \sin \varphi' & \cos \theta' \sin \varphi' & \cos \varphi' \\ \cos \theta' & -\sin \theta' & 0 \end{bmatrix}, \quad (4)$$

$$\mathbf{T}_2 = \begin{bmatrix} \cos \varphi \sin \theta & \sin \varphi \sin \theta & \cos \theta \\ -\sin \varphi & \cos \varphi & 0 \\ \cos \varphi \cos \theta & \sin \varphi \cos \theta & -\sin \theta \end{bmatrix}. \quad (5)$$

\mathbf{T}_2 is not equal to \mathbf{T}_1^{-1} since the angles (θ, φ) used in \mathbf{T}_2 can be expressed as function of (θ', φ') as follows

$$\theta = \arccos \left(\frac{a_x(\theta', \varphi')}{\sqrt{a_x^2(\theta', \varphi') + a_y^2(\theta', \varphi') + a_z^2(\theta', \varphi')}} \right)$$

$$\varphi = \arccos \left(\frac{a_x(\theta', \varphi')}{\sqrt{a_x^2(\theta', \varphi') + a_y^2(\theta', \varphi')}} \right) \quad (6)$$

with the unit vector \mathbf{a} , given by

$$\begin{bmatrix} a_x(\theta', \varphi') \\ a_y(\theta', \varphi') \\ a_z(\theta', \varphi') \end{bmatrix} = \mathbf{R}_m \begin{bmatrix} \sin \theta' \cos \varphi' \\ \sin \theta' \sin \varphi' \\ \cos \theta' \end{bmatrix}. \quad (7)$$

It must also be noticed that the spherical coordinates angles (θ', φ') of the requested far field calculated by FEKO takes discrete values. The new coordinate angles (θ, φ) in the main coordinate system $(\mathbf{e}_x, \mathbf{e}_y, \mathbf{e}_z)$ do not necessary match. For that reason an interpolation method will be required (see figure 4).

III. CHOICE OF THE ANTENN ELEMENT

We have seen before that the approximated method relies on the antenna element radiation characteristics that are taken into account in the array radiation characteristic. The method can be applied if the coupling between elements is low, thus an element that fulfills our design requirement has to be chosen to illustrate the approach. In our configuration, the choice of the antenna element is determined by different parameters. First limitations are resulting from the platform itself. The

antenna must radiate broadside, must be flat and must still radiate without ground plane. This prohibits all the antennas fed with a reference to a ground plane. Secondly, wideband performances of the array are limited by the size of the antenna since the elements must be half wavelength spaced. Finally, the conformation of the array leads to polarization and magnitude changes due to the various orientations of the elements. The choice of the antenna must be done after exploring these points.

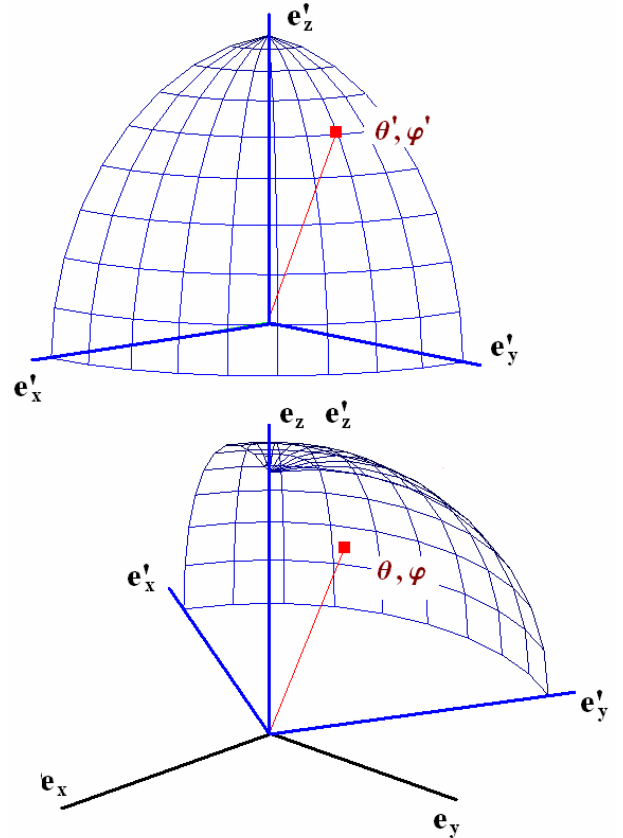


Fig. 4. Discretization of the spherical coordinate angles (θ', φ') in the (θ, φ) coordinate system of reference do not necessary match with the discretization of the main coordinate system.

Many designs exist for wideband and ultra wideband antenna [6], [7]. Some of them are low profile and research has been done recently to improve their performances. Archimedean spiral is a good candidate for wideband applications and has been chosen for our goal. It is usually not considered for phased array due to its size requirement [8]. Indeed, it radiates if its diameter D is larger or equal to λ_{\max}/π (with λ_{\max} the largest wavelength in the band). In addition, distance between array elements center to center, must be lower than half of the smallest wavelength of the bandwidth to avoid grating lobes when scanning. This leads to an element size less than or equal to $\lambda/2$. In consequence, condition

$2D \leq \lambda \leq \pi D$ must be fulfilled and the bandwidth is limited approximately to 1.5:1. Thus we can expect good functioning between 400 MHz and 600 MHz.

VSWR of a 0.27 m diameter spiral modeled with commercial software FEKO, calculated with a 200 Ω reference impedance, is plotted in figure 5. It can be observed that this antenna can radiate efficiently above 400 MHz. Its size corresponds to a distance between array elements center to center of 0.25 m, thanks to the curvature. Therefore, scanning can be obtained till the upper frequency, 600 MHz.

In a conformal configuration, all the elements do not radiate with the same field in a given direction because on their own radiation characteristic. Indeed the orientation of the elements depends on their position on the surface. Thus, it is required to know what is the radiation characteristic of the antenna element before including it in the approximated method in order to calculate the array radiation pattern.

Far field of the considered antenna is right hand circularly polarized (RHC) above the plane of the antenna and left hand circularly polarized (LHC) below (see figure 6). It has also the great advantage to radiate the same polarization over 180° (figure 6). That implies that the polarization characteristic of the conformal array will not be too much influenced by the orientations of the antenna elements.

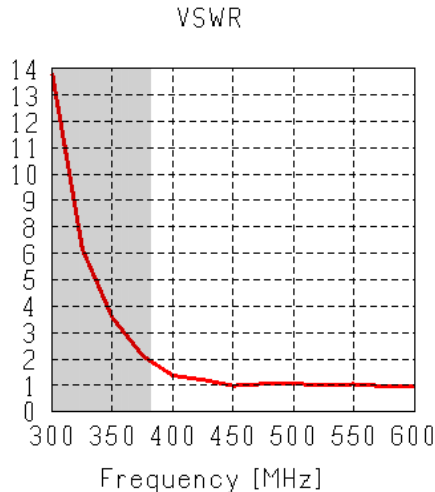


Fig. 5. VSWR of a spiral antenna with diameter of 0.27 m, calculated with 200 Ω reference impedance.

Gain in RHC polarization is plotted according to the φ angle in figure 7, at various frequencies. It can be seen that the more the frequency increases, the more the RHC polarized radiated field decreases, in the inward direction φ = 180°.

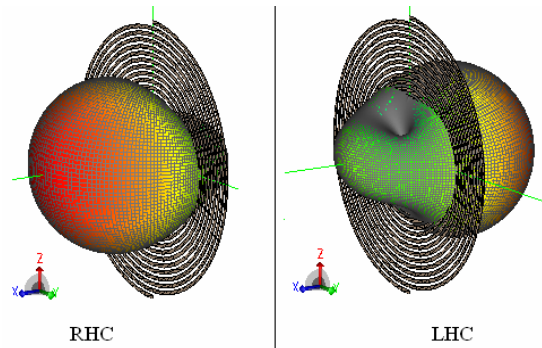


Fig. 6. 3D radiation pattern of spiral antenna. RHC polarized (right part) and LHC polarized (right part).

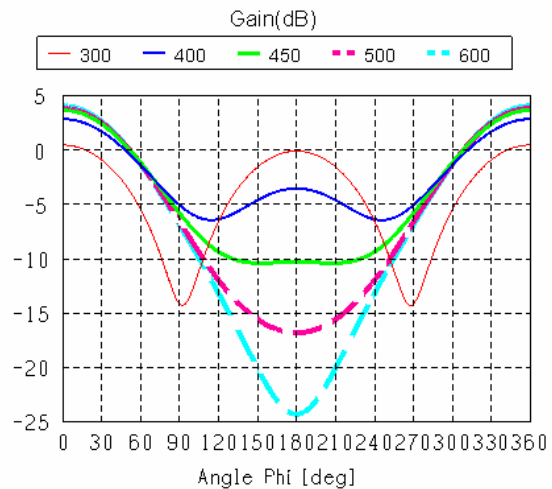


Fig. 7. Gain of RHC polarized component of the far field versus φ angle, at θ=90°, at various frequencies.

IV. STUDY OF COUPLING BETWEEN ARRAY ELEMENTS

Before using the approximated method, it is necessary to evaluate coupling between array elements, which have neglected in our approach. A circular 1D array with angle of curvature α and identical antennas (co-polar configuration) is considered (see figure 8). Only an eight-antenna array has been modeled with MoM, as it is time consuming. Coupling effects have been investigated based on the computation of the S parameters between spiral antenna ports. The influence of the frequency within a range of 300 MHz to 600 MHz as well as the curvature effect has been studied.

The S parameters for the planar case (0° of curvature) are shown in figure 9, whereas those for the conformal case (10° of curvature) are plotted in figure 10. Both figures show results for eight identical antennas radiating a RHC polarized far field in the outward direction. Angle of curvature α is the angle seen between

the element centers of two successive antennas from to the origin of the coordinate system.

It can be clearly noticed two different behaviors for the S parameters according to the frequency. The coupling between the element 1 (see figure 8) and an element close to it, i.e. S_{12} and S_{14} , roughly decreasing with the frequency, whereas an increase can be observed concerning the elements located in the opposite part of the array i.e. S_{16} and S_{18} . The rise appends at 450 MHz, where the distribution of the current along the two spiral arms exhibits also higher values.

When comparing the planar (figure 9) and the 10° conformal (figure 10) cases, few differences can be distinguished. We can conclude that a small angle of curvature like 10°, almost do not change radically the coupling between elements. The effect of curvature is clearer for the far element coupling S_{16} and S_{18} .

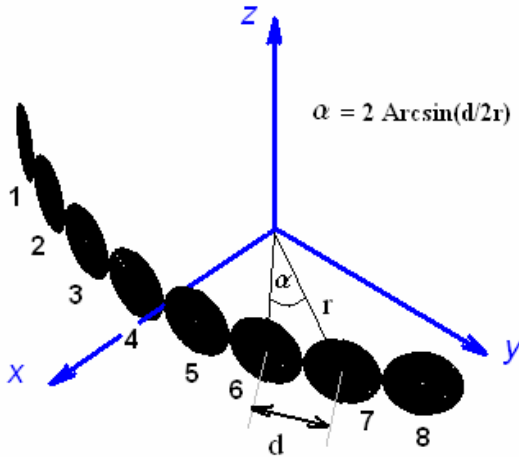


Fig. 8. Circular 1D conformal array configuration considered for the simulation. The 8 antennas are equally spaced. Angle of curvature α can vary.

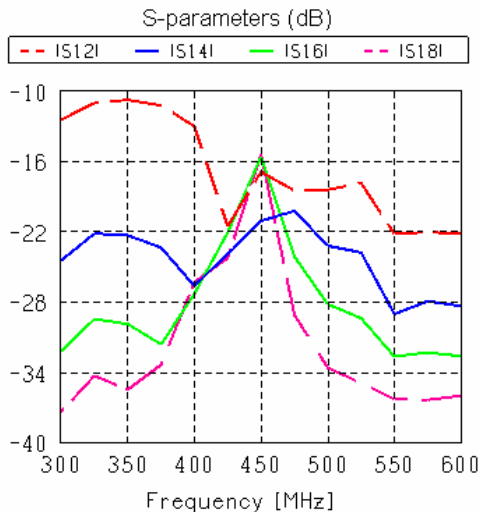


Fig. 9. S-parameters versus frequency. For the planar case $\alpha = 0^\circ$.

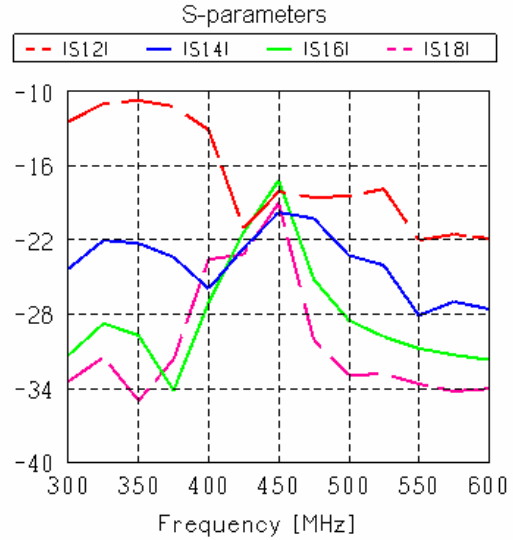


Fig. 10. S-parameters versus frequency. For the conformal case $\alpha = 10^\circ$.

V. COMPARISON OF METHODS

Radiation patterns obtained by the approximated method and FEKO are now compared for different frequencies and different angles of curvature in order to validate the approach. Figure 11 shows an example of radiation pattern plotted for RHC electric far field, at 450 MHz, with a curvature of 10°. On the upper part, can be seen the effects of the rotation of radiation pattern. Each radiation pattern corresponds to an antenna element that has been rotated according to its orientation, in the $\theta = 90^\circ$ plane.

The middle part depicts conformal array radiation pattern that corresponds to a uniformly excited array with omnidirectional sources. It emphasizes the effects due to the geometry of the conformal array itself. Those effects are combined in the radiation pattern, given by the approximated method, using equations (1) and (3), and can be observed in the lower part of figure 11, which shows the comparison between the two methods. It can be observed that the radiation pattern due to point sources has been reshaped by each antenna element radiation characteristic to give the final radiation pattern.

The two methods have been compared for frequencies within the range of 400 MHz to 600 MHz and for 0°, 5°, and 10° of curvature. Some examples are given below. Figures 12 and 13 show the comparison of two methods for the planar case, at 400 MHz and 600 MHz, respectively. Figures 14 and 15 show the results for the 10° conformal case, at 400 MHz and 600 MHz, respectively.

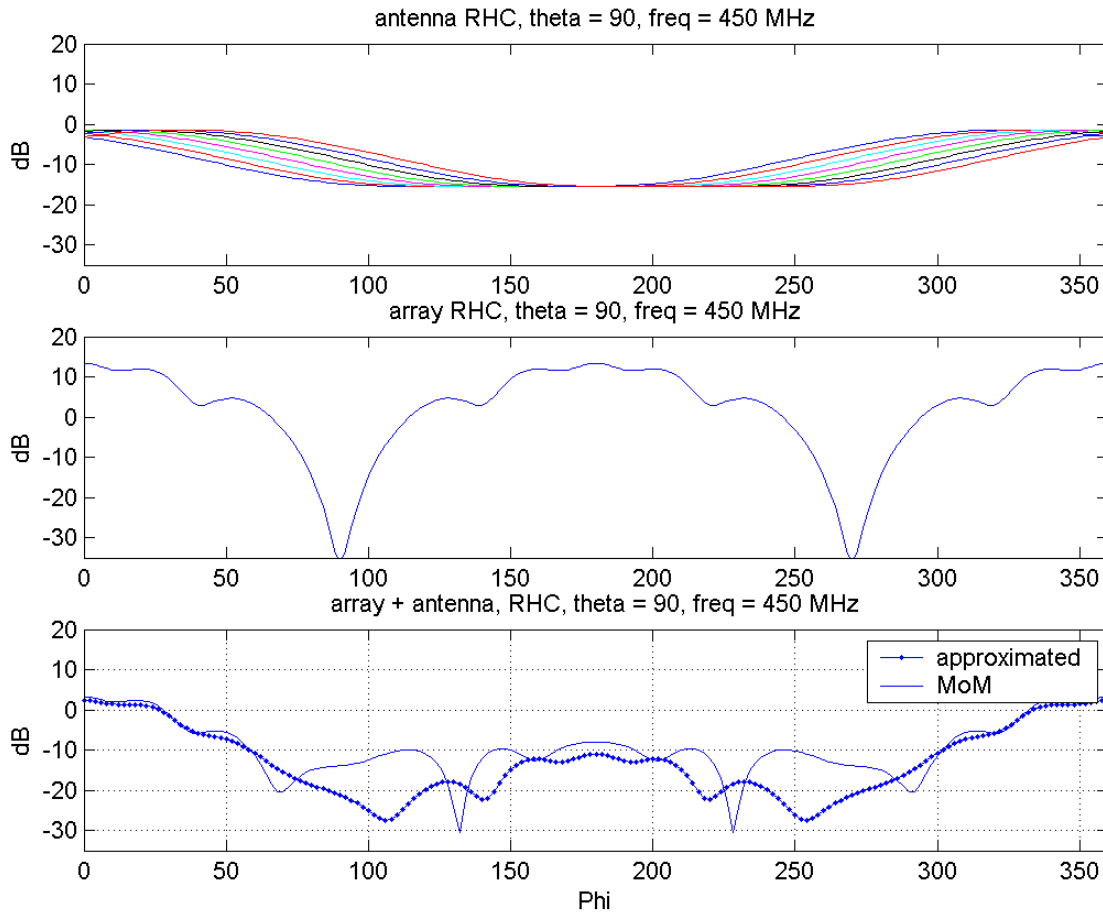


Fig. 11. RHC electric far field at 450 MHz with curvature of 10° . Top: 8 antenna rotated radiation patterns. Middle: uniformly excited conformal array with omni-directional sources. Bottom: comparison between the two methods.

As it can be seen in figures 12 to 15, reconstruction of the main lobe at $\varphi=0^\circ$, is fulfilled for frequencies within the band 400 MHz to 600 MHz. Inward lobe, at $\varphi=180^\circ$, exhibits more important differences between the two methods, especially when the radiation of the isolated element in this direction is particularly low. When comparing the planar case with the conformal case, it can be noticed that this difference for the inward lobe happens in both cases. Moreover, both cases exhibit higher differences at 600 MHz. Therefore we can conclude that this effect comes from the radiation characteristic of the isolated element itself when used in the approximated method.

We highlight before that at 450 MHz behavior of coupling strongly changes. Nevertheless, no specific effect has been noticed concerning the differences between exact method and approximated method (see figure 11), except that stronger differences can be distinguished around $\varphi=90^\circ$ and $\varphi=270^\circ$ corresponding to the lowest radiation direction of the antenna element (endfire direction). So, for the considered array of eight spiral antennas, in the conformal case as in the planar

case, it is possible to obtain the shape and level of the main lobe simply by summing the contribution of each antenna element, including the orientation of each one.

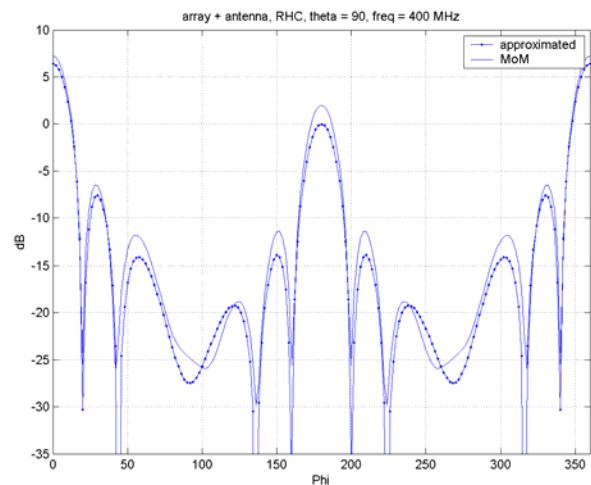


Fig. 12. Two methods comparison for 0° curvature (planar case) at 400 MHz.

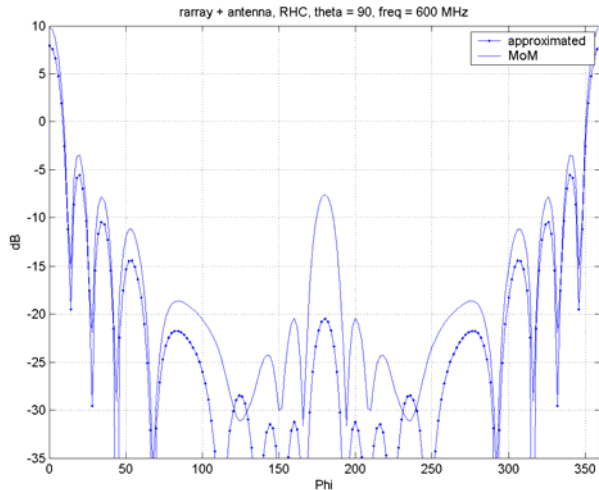


Fig. 13. Two methods comparison for 0° curvature (planar case) at 600 MHz.

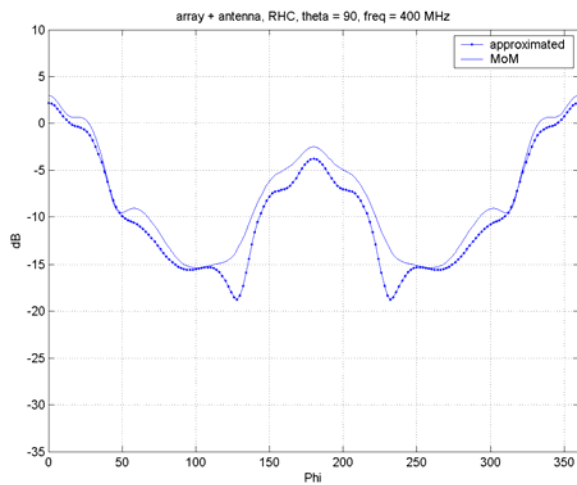


Fig. 14. Two methods comparison for 10° curvature (conformal case) at 400 MHz.

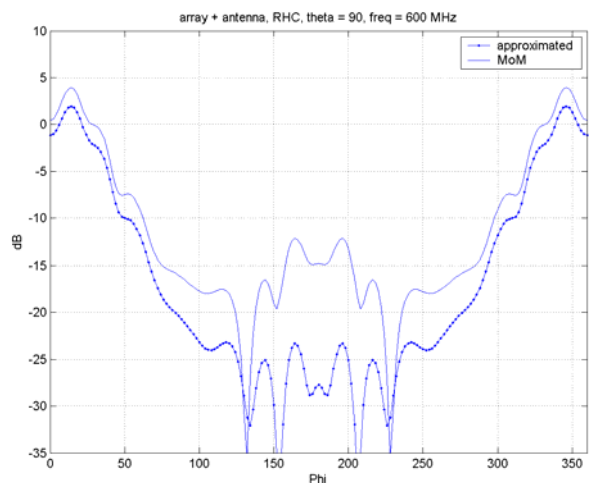


Fig. 15. Two methods comparison for 10° curvature (conformal case) at 600 MHz.

VI. CONCLUSIONS

An approximated method has been presented to solve the time consuming issue of a large array modeled with MoM. It has been illustrated with a specific configuration: a conformal spiral antenna array that achieves wideband performances on an inflatable structure. The approximated method neglects the coupling and is based on the summation that includes the rotation of each element radiation characteristic. It has the advantage of taking into account the vectorial nature of the array radiation characteristic. For the chosen design, coupling between elements has been studied, and the curvature of the array seems to not influence significantly its value. Finally, validation of the radiation patterns obtained by the approximated method has been performed by comparing with a full wave method. It has shown that main lobe reconstruction is fulfilled, but differences still remain for the inward lobe because of low levels in that direction. However, this method allows to predict the shape of array radiation pattern in a very simple and general way. It provides also an interesting tool that can be used as a first approximation for conformal array analysis.

REFERENCES

- [1] Integrated Sensor Is Structure, "Proposer information pamphlet", DARPA, Sept. 2003
- [2] C. A. Balanis, *Antenna theory, analysis and design*, Wiley; 2 Edition, ISBN: 0471592684, May 1996.
- [3] R. C. Hansen, *Microwave Scanning Antennas*, Vol. II, Academic Press, New York and London, 1966.
- [4] EM Software & Systems-S.A., *FEKO User's Manual*, 32 Techno Lane, Technopark, Stellenbosch, 7600 South Africa, June 2004.
- [5] A. Gray, *A Treatise on Gyrostatics and Rotational Motion*, MacMillan, London, 1918.
- [6] S. - Y. Suh, "A comprehensive investigation of new planar wideband antennas", PhD thesis in Electrical Engineering, Virginia Polytechnic Institute and State University, July 2002.
- [7] E. Caswell, "Design and analysis of star spiral with application to wideband arrays with variable element sizes", PhD thesis in Electrical engineering, Virginia Polytechnic institute and state University, Dec., 2001.
- [8] H. Steykal, J. Ramprecht, and H. Holter, "Spiral element broad band phased array", *IEEE Trans. Antennas Propagation*, Vol. 53, No. 8, pp. 2558-2562, August 2005.